Journal of Superconductivity and Novel Magnetism (2021) 34:617–622
https://doi.org/10.1007/s10948-020-05732-7

ORIGINAL PAPER

Manifestation of Magnetic Characteristics of Zinc Ferrite Nanoparticles Using the Langevin Function

Elangbam Chitra Devi[1] · Shougaijam Dorendrajit Singh[1]

Received: 16 July 2020 / Accepted: 17 October 2020 / Published online: 7 November 2020

Abstract

Zinc ferrite ($ZnFe_2O_4$) nanoparticles were prepared by chemical co-precipitation method. Structural characterization was performed using X-ray diffraction (XRD) and transmission electron microscopy (TEM). Formation of spinel phase was confirmed from XRD studies. Crystallite size and lattice constant of the prepared sample were calculated. TEM images reveal spherical-shaped particles with nanosized distribution. Room temperature magnetic hysteresis loop was recorded using vibrating sample magnetometer (VSM). The magnetization loops exhibit a very narrow loop and behave like superparamagnetic nature. Using the Langevin function, the magnetic behaviour of the prepared nanoparticles was investigated. From the curve fitting, saturation magnetization and reduced magnetization were determined. As-prepared sample was further annealed at three different temperatures namely 800 °C, 1000 °C, and 1200 °C for 2-h duration. The effects of annealing on the structural and magnetic properties were further investigated using XRD and VSM. The observed results on the magnetic characteristics of $ZnFe_2O_4$ and applicability of the Langevin function are being discussed.

Keywords Magnetization curves · Zinc ferrite · Superparamagnetism · Langevin function · Spinel ferrites

1 Introduction

Magnetic materials occupy an important place in different technological developments. They are extensively investigated and being applied in different fields such as memory devices, biomedical applications, polluted water treatment technologies, and microwave devices [1–3]. Bringing them to various applications requires a good knowledge of their characteristic properties which necessitates the detail understanding of the magnetization curves. Different researchers reported theoretical models with an attempt to describe different kinds of magnetic materials [4–6]. On the other hand, these models are being tested and applied to a variety of materials by many experimentalists [7–11]. It includes different forms of law of approach to saturation magnetization, the Langevin function for paramagnetic and superparamagnetic materials. They are reported to be used to investigate the magnetic characteristics of different kinds of magnetic materials. Fine magnetic nanoparticles arouse great interest to researchers because of their superparamagnetic properties and hence their applicability of different areas. Among them, $ZnFe_2O_4$ nanoparticles are also reported to be an important one having superparamagnetic properties. $ZnFe_2O_4$ belongs to the category of spinel ferrites which occupies an important class of magnetic materials [1, 12]. Spinel ferrites have a unit cell composed of 32 oxygen atoms in a cubic closest packing, leaving behind two interstitial sites, namely the tetrahedral (A) and octahedral (B) sites available for the cations. Normally, for $ZnFe_2O_4$, Zn^{2+} occupies A sites and hence belongs to the category of normal spinel ferrites. Different synthesis routes such as solid state method, sol gel, auto-combustion, hydrothermal, and co-precipitation method have been reported for the synthesis of spinel ferrites [13–17]. Their properties in general are reported to be dependent on their synthesis methods as well as other processing conditions such as pH of the reaction, and heat treatment temperature and duration [17–19].

In this work, we investigate the structural and magnetic properties of fine nanoparticles of $ZnFe_2O_4$ along with the effect of annealing temperature on their characteristic properties. Also, we report studies on the magnetization data using the Langevin function and determination of the intrinsic magnetic parameters associated with them.

✉ Elangbam Chitra Devi
elangbam_chitra@rediffmail.com

[1] Department of Physics, Manipur University, Canchipur, Imphal, Manipur 795003, India

2 Experimental Details

2.1 Materials and Method

Zinc ferrite nanoparticles were prepared by a simple co-precipitation method. The starting materials were zinc (II), chloride (dry $ZnCl_2$), iron (III), chloride anhydrous ($FeCl_3$), and sodium hydroxide (NaOH). Aqueous solution of 0.5 M $MnCl_2$ and 1 M $FeCl_3$ was mixed at 60 °C with continuous stirring. It was then added to 0.6 M NaOH solution which was initially heated at 80 °C with continuous stirring. The solution was maintained at 85 °C for 1 h. The precipitate obtained was centrifuged and washed several times with distilled water and dried at 80 °C. Then, the product so obtained was grounded into fine powders. Furthermore, the sample was annealed at three different temperatures, namely 800 °C, 1000 °C, and 1200 °C, for 2 h in open air. The sample was then finally subjected to different characterizations.

2.2 Characterization

The phase structure of the prepared $ZnFe_2O_4$ was studied by X-ray diffraction (XRD) with Cu-K_α radiation. TEM images for as-prepared sample were recorded with a TEM 200 kV (JEM-2100). The magnetic study was carried out using vibrating sample magnetometer (VSM Lakeshore 7410). All the abovementioned measurements were conducted at room temperature.

3 Result and Discussion

3.1 XRD

The XRD patterns of the prepared $ZnFe_2O_4$ nanoparticles are presented in Fig. 1. It confirms the formation of spinel phase of $ZnFe_2O_4$ corresponding to the standard reference pattern ICDD-01-070-6491. The average crystallite size, D, was calculated using the Scherrer formula

$$D = \frac{k\lambda}{\beta\cos\theta} \tag{1}$$

where λ is the wavelength of the X-ray used, k is a constant related to the shape of the particles, and β being full width at half maximum of the diffraction peak. Instrumental broadening was determined using standard silicon powder. The corrected full width at half maximum value, β, was determined using the relation $\beta^2 = \beta_o^2 - \beta_i^2$, where β_o and β_i are observed full width at half maximum and full width at half maximum due to instrumental broadening respectively. Taking $\lambda = 0.15406$ nm, $k = 0.9$, and using β of the most intense peak in the XRD pattern, average crystallite sizes were

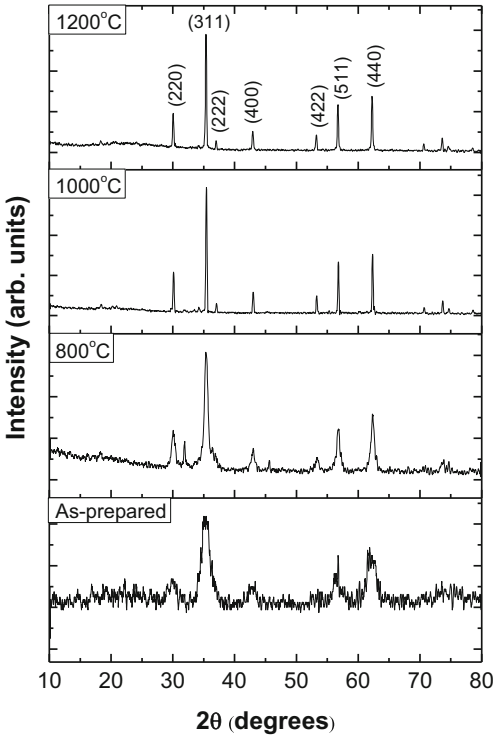

Fig. 1 XRD pattern of as-prepared and annealed $ZnFe_2O_4$ nanoparticles

calculated which are listed in Table 1. It was found to be 7 nm for as-prepared and 21, 103, and 106 nm for annealed at 800, 1000, and 1200 °C, respectively. The characteristic broad peaks of the XRD pattern of as-prepared $ZnFe_2O_4$ also depict its nanosized distribution. On annealing and also with increasing annealing temperature, a remarkable increase in the average crystallite size characterized with narrow and intense peaks can be seen. Using five most intense peaks from the XRD data, lattice constant, a, were determined using the equation

$$a = d\sqrt{h^2 + k^2 + l^2} \tag{2}$$

where d is the inter planer spacing and h, k, and l being the miller indices of the diffraction peaks. The calculated values of lattice constant are given in Table 1. Lattice constant of as-prepared sample shows a larger value as compared to the annealed samples. This may have arisen due to the size effects as owing to its nanosized nature, the structural perturbation may have resulted. Similar results have also been found in the literature [20]. Also, a remarkable contribution may come from the variation in the cationic distribution. It is reported that $ZnFe_2O_4$ in nanoregime is found to have mixed spinel structure while in bulk has normal spinel structure. The processing parameters like annealing temperature have an impact on the cation distribution and hence lattice constant of $ZnFe_2O_4$. The combined effects of the above mentioned factors may have resulted in the variation of lattice constant of $ZnFe_2O_4$ with different annealing temperature.

Table 1 Crystallite size (nm), lattice constant (Å), M_s (emu/g), H_c (Oe), M_r (emu/g), magnetic moment, μ (μ_B), R^2, and χ^2 values of as-prepared and annealed $ZnFe_2O_4$ nanoparticles

Annealing temperature (°C)	Crystallite size (nm)	Lattice constant (Å)	M_s (emu/g)	H_c (Oe)	M_r (emu/g)	Magnetic moment, μ (μ_B)	R^2	χ^2
As-prepared	7	8.512	13.30 ± 0.12	38	0.01	550	0.999	0.007
800	21	8.410	9.15 ± 0.07	58	0.03	739	0.999	0.006
1000	103	8.404	4.46 ± 0.05	58	0.02	676	0.998	0.002
1200	106	8.416	3.72 ± 0.07	69	0.02	530	0.998	0.001

3.2 TEM Studies

Bright field TEM images at different magnification of the as-prepared $ZnFe_2O_4$ are shown in Fig. 2(a–d). The micrographs depict the formation of almost spherical nanoparticles around an average size of 10 nm. So, the average size is found to be approximately in agreement with the crystallite size obtained from the XRD studies. Lattice fringes of the individual crystallites are also observed in high-resolution image (Fig. 2(c)) depicting the crystalline nature of the nanoparticles. The selected area electron diffraction (SAED) pattern is shown in Fig. 2(d). It can be seen that the SAED pattern consists of spots and rings which clearly indicates the polycrystalline nature of the prepared $ZnFe_2O_4$ nanoparticles as the rings and spots are resulted from the random orientation of the crystallites of the nanoparticles [21].

3.3 Magnetic Studies

Room temperature magnetization loops of $ZnFe_2O_4$ are shown in Fig. 3. The values of coercivity, H_c, and retentivity, M_r, of the prepared samples obtained from the magnetization loops are listed in Table 1. All the prepared samples possess small values of retentivity lying in the range of 0.01 to 0.03 emu/g. Coercivity of the prepared samples increases with the increase in annealing

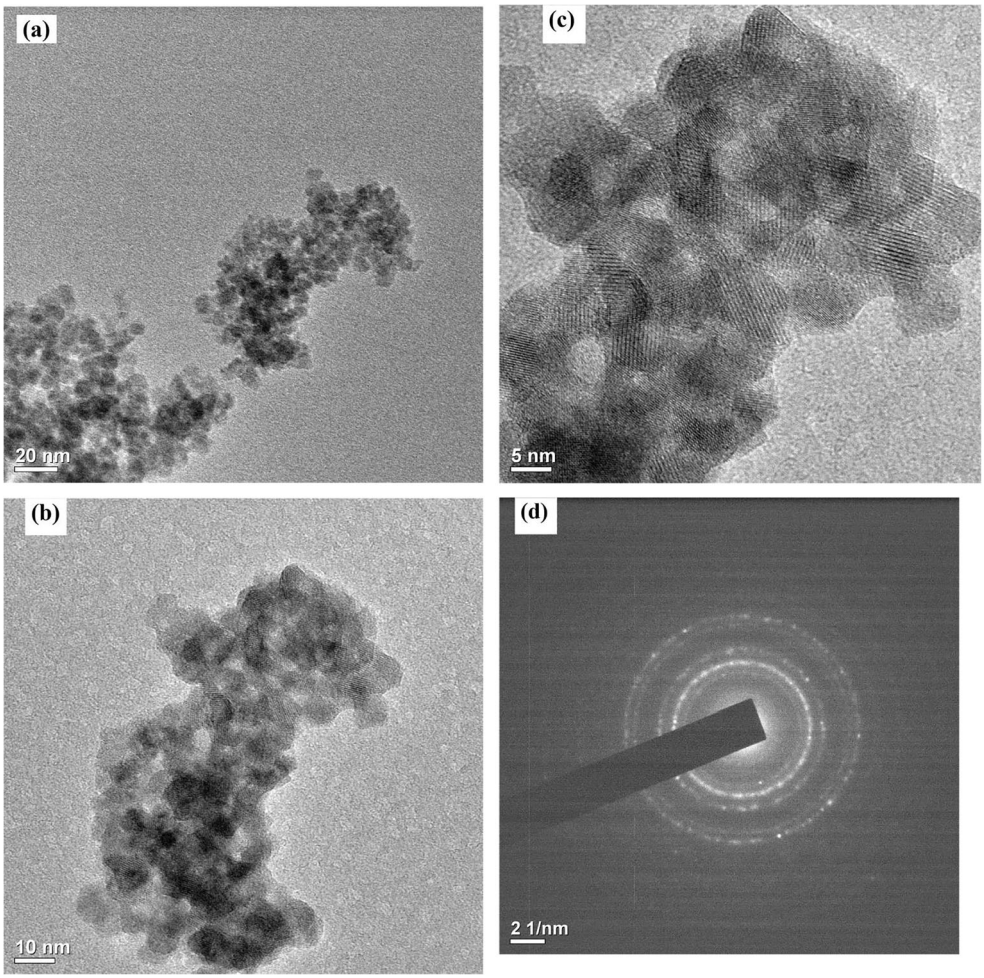

Fig. 2 TEM images at different magnification (a)–(c) and selected area electron diffraction pattern (d) of as-prepared $ZnFe_2O_4$ nanoparticles

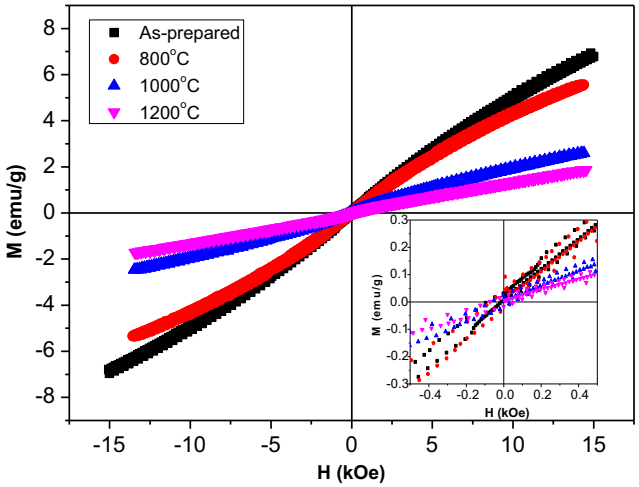

Fig. 3 MH loops of as-prepared and annealed $ZnFe_2O_4$ nanoparticles

temperature. It may be readily understood in terms of variation of size of prepared samples. Coercivity of nanoparticles has a striking dependence on their size. As the size decreases, coercivity increases in the multi-domain region, reaches a maximum at a critical diameter where particles become single domain and then decrease with further decrease in the size [4]. On the other hand, this observed behaviour gives an indication of the prepared samples in the single-domain regime. It can be seen that magnetization loops exhibit very narrow loops. As-prepared sample exhibits higher magnetization as compared to annealed samples and magnetization decreases with increasing annealing temperature. On annealing and also with the increase of annealing temperature, the magnetization loops exhibit a transition of slightly S-shaped (in the case of as-prepared) to a linear nature (in the case of annealed) can be observed. To further investigate the nature of the magnetic characteristics, the magnetization data is fitted with the Langevin function which is usually described as

$$M = M_s\left[\coth\left(\frac{\mu H}{k_B T}\right) - \left(\frac{k_B T}{\mu H}\right)\right] \quad (3)$$

where μ, k_B, H, T, and M_s being the reduced magnetic moment, Boltzmann constant, applied magnetic field, temperature, and saturation magnetization, respectively [22, 23].

Magnetization data fitted with the Langevin function are shown in Fig. 4(a–d). It can be clearly seen that the magnetization data of $ZnFe_2O_4$ fits well with the Langevin function. The goodness of fitting parameters R^2 and χ^2 values along with the fitted parameters are given in Table 1. The closeness of the R^2 value to unity confirms the good fitting of the experimental data with the Langevin equation. Excellent fitting of the magnetization data

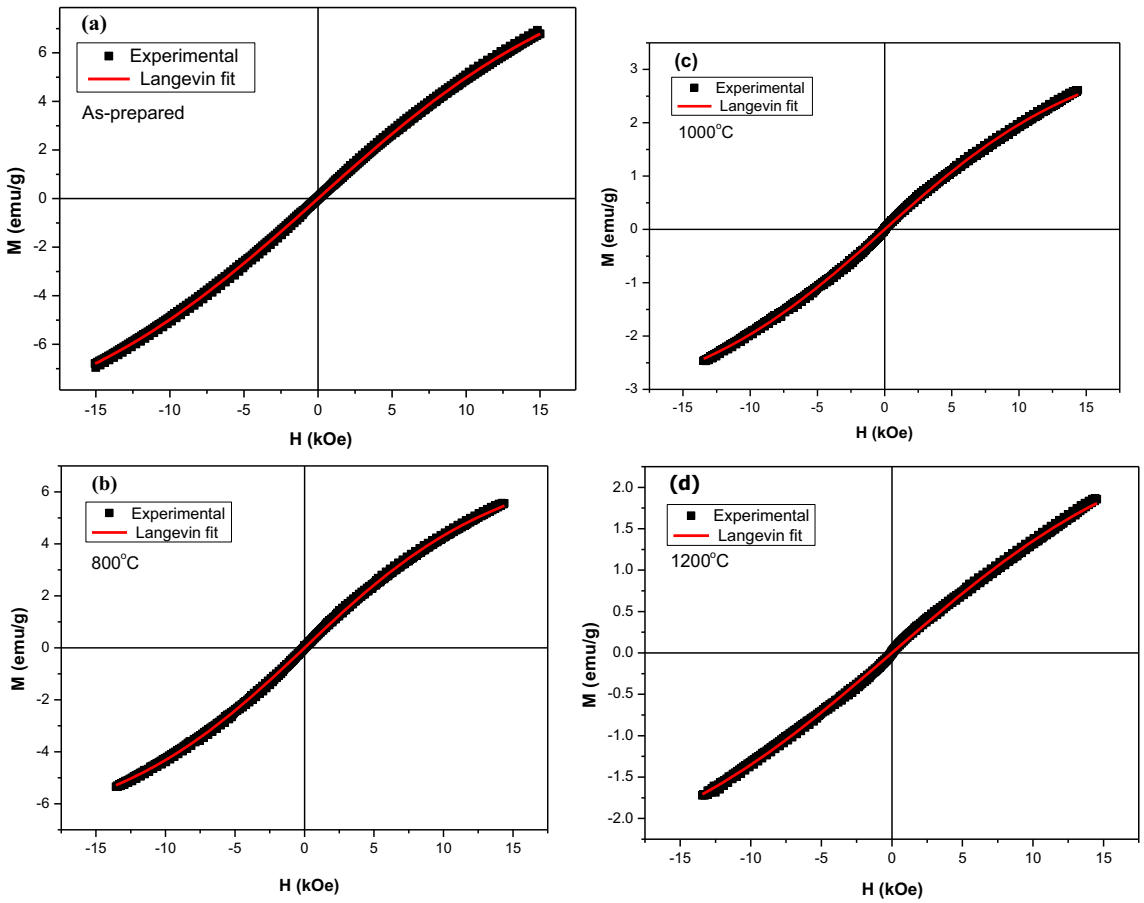

Fig. 4 (a)–(d) Fitting of magnetization data of as-prepared and annealed $ZnFe_2O_4$ nanoparticles using the Langevin function

with the Langevin function implies that prepared nanoferrites behave like superparamagnetic or paramagnetic nature. Basically, paramagnetic materials possess very weak magnetic moments but in the absence of an external magnetic field, they do not retain any net magnetization because of the randomizing thermal effects. With response to an external applied field, their magnetization curves are characterized by a weak positive and linear magnetization and on removal of the field, magnetization becomes zero. Superparamagnetic materials are usually considered a system of widely spaced or isolated and non-interacting single-domain particles such that magnetic moments of the particles act independently along with instability of magnetization due to thermal agitation. Similar to paramagnetic materials, thermal energy randomizes the magnetization in superparamagnetic materials in the absence of an applied field. However, on application of an external field, they tend to align along the field direction with a much higher magnetization value compared to paramagnetic materials. Owing to its similar behaviour with paramagnetic materials, the Langevin function is reported to be applied to study the magnetization curves of superparamagnetic materials [23, 24]. It is found to apply in different types of materials such as antiferromagnetic nickel oxide nanoparticles, $CaFe_2O_4$, Fe_3O_4, and composites of bismuth ferrites and nickel zinc ferrites [22, 23, 25, 26]. From the curve fitting, saturation magnetization and reduced magnetic moment were determined and are given in Table 1. It can be seen that saturation magnetization decreases with increasing annealing temperature. The observed result may be understood in terms of cation distribution of $ZnFe_2O_4$. It has been reported that $ZnFe_2O_4$ in bulk form belongs to the category of normal spinel ferrite in which Zn^{2+} ions occupy tetrahedral (A) sites and trivalent Fe^{3+} ions occupy octahedral (B) sites of the spinel structure which is usually represented as $(Zn_1)_A$ $[Fe_2]_B$ O_4 and behaves like paramagnet [27, 28]. However, in the case of $ZnFe_2O_4$ nanoparticles, partial occupancy of Fe^{3+} in A sites occurs that is $(Zn_{1-x}Fe_x)_A$ $[Zn_x\ Fe_{2-x}]_B$ O_4 and hence results in an enhanced magnetic moment [27, 28]. Upon the increase in the inversion degree x, the magnetization value changes and hence ferrimagnetic behaviour of nanocrystalline $ZnFe_2O_4$. Although the cationic distribution strongly depends on the synthesis method and the processing conditions, it is commonly reported that the low-temperature preparation methods usually have higher inversion degree and hence higher saturation magnetization [20]. The reduced magnetic moment is expressed as the product of volume of the particle and the saturation magnetization [22]. And for spherical particles of diameter D, it is usually given by

$$\mu = \frac{4}{3}\,\pi\left(\frac{D}{2}\right)^3 M_s \tag{4}$$

Reduced magnetic moment of prepared $ZnFe_2O_4$ nanoparticles was found to be in the range 530–739 μ_B. An irregular trend in reduced magnetic moment with variation of annealing temperature can be seen. This may have resulted from two competitive factors as saturation magnetization decreases while size increases with increasing annealing temperature.

Ideally speaking, coercivity is zero for superparamagnetic nanoparticles, but may not be necessarily zero in the case of real samples which are also reported by many researchers [25, 26, 29–31]. In addition, negligible coercivity is not the only criteria for superparamagnetism, but well-fitting of magnetization data with the Langevin function is an indicator of superparamagnetism which is also reported by different researchers [29, 30, 32]. Also, in the case of annealed samples, coercivity is not zero, but their linear characteristics, well-fitting to the Langevin function, negligible retentivity depicts paramagnetic behaviour. Very small values of retentivity (in the range of 0.01–0.03 emu/g) and well-fitting of the Langevin function was common in all the samples but differences in saturation magnetization values ($M_s = 13.30 \pm 0.12$ for as-prepared and $M_s = 3.72 \pm 0.07$ for 1200 °C annealed $ZnFe_2O_4$) were observed. This implies a clear transition from superparamagnetic to paramagnetic nature of $ZnFe_2O_4$ samples on annealing and with increasing annealing temperature.

4 Conclusion

Spinel phase $ZnFe_2O_4$ nanoparticles were successfully synthesized by a low-temperature co-precipitation method. Average crystallite size of the as-prepared $ZnFe_2O_4$ calculated using XRD was found to be 7 nm. TEM reveals spherical-shaped nanoparticles. On subjecting to annealing temperature of 800, 1000, and 1200 °C, crystallite size increases to 21, 103, and 106 nm, respectively. Coercivity was observed to be increased with the increase of annealing temperature. Increase in coercivity with increasing size of the prepared nanoparticles gives an indication of the prepared samples in the single-domain regime. Excellent fitting of magnetization data with the Langevin function was observed for all the prepared samples. Saturation magnetization and reduced magnetic moment were obtained from the curve fitting. Saturation magnetization decreases with increasing annealing temperature which may have arisen due to change in the inversion degree of the cation distribution. As-prepared samples seem to possess a superparamagnetic behaviour which transforms to paramagnetic one with increasing annealing temperature. The overall results show that magnetization data of $ZnFe_2O_4$nanoparticles can be successfully described by the Langevin function.

Acknowledgements Elangbam Chitra Devi is thankful to the University Grants Commission, New Delhi, India, for the award of Dr. D.S. Kothari Post-Doctoral Fellowship (Award No. F. 4-2/2006(BSR)/PH/18-19/0090). Authors are grateful to CIF, IIT Guwahati for VSM measurements and SAIF, NEHU for TEM measurements.

References

1. Goldman, A.: Modern Ferrite Technology. Springer, USA (2006)
2. Kefeni, K.K., Mamba, B.B., Msagati, T.A.M.: Application of Spinel Ferrite Nanoparticles in Water and Wastewater Treatment: a Review, vol. 188, p. 399 (2017)
3. Harres, A., Mikhov, M., Skumryev, V., De Andrade, A.M.H., Schmidt, J.E., Geshev, J.: Criteria for saturated magnetization loop. J. Magn. Magn. Mater. **402**, 76 (2016). https://doi.org/10.1016/j.jmmm.2015.11.046
4. Cullity, B.D., Graham, C.D.: Introduction to Magnetic Materials (Google eBook). John Wiley & Sons, Hoboken, New Jersey (2011)
5. Akulov, N.S.: Über den Verlauf der Magnetisierungskurve in starken Feldern. Zeitschrift für Phys. **69**, 822–831 (1931)
6. Brown, W.F.: Theory of the approach to magnetic saturation. Phys. Rev. **58**, 736–743 (1940). https://doi.org/10.1103/PhysRev.58.736
7. Devi, E.C., Soibam, I.: Magnetic properties and law of approach to saturation in Mn-Ni mixed nanoferrites. J. Alloys Compd. **772**, 920–924 (2019). https://doi.org/10.1016/j.jallcom.2018.09.160
8. Devi, E.C., Soibam, I.: Law of approach to saturation in Mn–Zn ferrite nanoparticles. J. Supercond. Nov. Magn. **32**, 1293–1298 (2019). https://doi.org/10.1007/s10948-018-4823-4
9. Devi, E.C., Soibam, I.: Journal of Magnetism and Magnetic Materials Tuning the magnetic properties of a ferrimagnet. J. Magn. Magn. Mater. **469**, 587–592 (2019). https://doi.org/10.1016/j.jmmm.2018.09.034
10. Komogortsev, S.V., Iskhakov, R.S.: Law of approach to magnetic saturation in nanocrystalline and amorphous ferromagnets with improved transition behavior between power-law regimes. J. Magn. Magn. Mater. **440**, 213–216 (2017). https://doi.org/10.1016/j.jmmm.2016.12.145
11. McCallum, R.W.: Determination of the saturation magnetization, anisotropy field, mean field interaction, and switching field distribution for nanocrystalline hard magnets. J. Magn. Magn. Mater. **292**, 135–142 (2005). https://doi.org/10.1016/j.jmmm.2004.10.105
12. Smit, J., Wijn, H.P.: Ferrites. Cleaver-Hume Press Ltd., London (1959)
13. Devi, E.C., Soibam, I.: Effect of Zn doping on the structural, electrical and magnetic properties of MnFe2O4 nanoparticles. Indian J. Phys. **91**, 861–867 (2017). https://doi.org/10.1007/s12648-017-0981-7
14. Devi, E.C., Soibam, I.: An investigation on the optical band gap and Ac conductivity of Mn-Zn nanoferrites. J. Supercond. Nov. Magn. **31**, 1183 (2017). https://doi.org/10.1007/s10948-017-4294-z
15. Chinnasamy, C.N., Narayanasamy, A., Ponpandian, N., Chattopadhyay, K., Shinoda, K., Jeyadevan, B., Tohji, K., Nakatsuka, K., Furubayashi, T., Nakatani, I.: Mixed spinel structure in nanocrystalline NiFe2O4. Phys. Rev. B - Condens. Matter Mater. Phys. **63**, 2–7 (2001). https://doi.org/10.1103/PhysRevB.63.184108
16. Hu, P., Yang, H., Pan, D., Wang, H., Tian, J., Zhang, S., Wang, X., Volinsky, A.A.: Heat treatment effects on microstructure and magnetic properties of Mn–Zn ferrite powders. J. Magn. Magn. Mater. **322**, 173–177 (2010). https://doi.org/10.1016/j.jmmm.2009.09.002
17. Ranjith Kumar, E., Arunkumar, T., Prakash, T.: Heat treatment effects on structural and dielectric properties of Mn substituted CuFe2O4 and ZnFe2O4 nanoparticles. Superlattice. Microst. **85**, 530 (2015). https://doi.org/10.1016/j.spmi.2015.06.016
18. Devi, E.C., Soibam, I.: A correlated structural and electrical study of manganese ferrite nanoparticles with variation in sintering temperature. Mod. Phys. Lett. B. **31**, 1750236 (2017). https://doi.org/10.1142/S0217984917502360
19. Hu, P., Yang, H.-b., Pan, D.-a., Wang, H., Tian, J.-j., Zhang, S.-g., Wang, X.-f., Volinsky, A.A.: Heat treatment effects on microstructure and magnetic properties of Mn-Zn ferrite powders. J. Magn. Magn. Mater. **322**, 173 (2010). https://doi.org/10.1016/j.jmmm.2009.09.002
20. Choi, E.J., Ahn, Y., Hahn, E.J.: Size dependence of the magnetic properties in superparamagnetic zinc-ferrite nanoparticles. J. Korean Phys. Soc. **53**, 2090–2094 (2008). https://doi.org/10.3938/jkps.53.2090
21. Egerton, R.F.: Physical Principles of Electron Microscopy. (2005)
22. Lal, G., Punia, K., Dolia, S.N., Alvi, P.A., Dalela, S., Kumar, S.: Rietveld refinement, Raman, optical, dielectric, Mössbauer and magnetic characterization of superparamagnetic fcc-CaFe2O4 nanoparticles. Ceram. Int. **45**, 5837–5847 (2019). https://doi.org/10.1016/j.ceramint.2018.12.050
23. Manohar, A., Krishnamoorthi, C.: Low curie-transition temperature and superparamagnetic nature of Fe3O4 nanoparticles prepared by colloidal nanocrystal synthesis. Mater. Chem. Phys. **192**, 235–243 (2017). https://doi.org/10.1016/j.matchemphys.2017.01.039
24. Tiwari, S.D., Rajeev, K.P.: Effect of distributed particle magnetic moments on the magnetization of NiO nanoparticles. Solid State Commun. **152**, 1080–1083 (2012). https://doi.org/10.1016/j.ssc.2012.03.003
25. Abdul Khadar, M., Biju, V., Inoue, A.: Effect of finite size on the magnetization behavior of nanostructured nickel oxide. Mater. Res. Bull. **38**, 1341–1349 (2003). https://doi.org/10.1016/S0025-5408(03)00139-9
26. Dhanalakshmi, B., Vivekananda, K.V., Rao, B.P., Rao, P.S.V.S.: Superparamagnetism in Bi0.95Mn0.05FeO3 – Ni0.5Zn0.5Fe2O4 multiferroic nanocomposites. Phys. B Condens. Matter. **571**, 5–9 (2019). https://doi.org/10.1016/j.physb.2019.06.058
27. Singh, R., Jaromir, Y., Ivo, H., Kozakova, Z., Palou, M., Barton, E.: Magnetic Properties of ZnFe 2 O 4 Nanoparticles Synthesized by Starch-Assisted Sol – Gel Auto-combustion Method. **28**, 1417 (2014). https://doi.org/10.1007/s10948-014-2870-z
28. Kavas, H., Baykal, A., Toprak, M.S., Köseoğlu, Y., Sertkol, M., Aktaş, B.: Cation distribution and magnetic properties of Zn doped NiFe2O4 nanoparticles synthesized by PEG-assisted hydrothermal route. J. Alloys Compd. **479**, 49–55 (2009). https://doi.org/10.1016/j.jallcom.2009.01.014
29. Keshri, S., Biswas, S., Wiśniewski, P.: Studies on characteristic properties of superparamagnetic La0.67Sr0.33-xKxMnO3 nanoparticles. J. Alloys Compd. 656, 245–252 (2016). https://doi.org/10.1016/j.jallcom.2015.09.176
30. Aguiló-Aguayo, N., Inestrosa-Izurieta, M.J., García-Céspedes, J., Bertran, E.: Morphological and magnetic properties of superparamagnetic carbon-coated Fe nanoparticles produced by arc discharge. J. Nanosci. Nanotechnol. **10**, 2646–2649 (2010). https://doi.org/10.1166/jnn.2010.1420
31. Lal, G., Punia, K., Dolia, S.N., Alvi, P.A., Choudhary, B.L., Kumar, S.: Structural, cation distribution, optical and magnetic properties of quaternary Co0.4+xZn0.6-xFe2O4 (x = 0.0, 0.1 and 0.2) and Li doped quinary Co0.4+xZn0.5-xLi0.1Fe2O4 (x = 0.0, 0.05 and 0.1) nanoferrites. J. Alloys Compd. **828**, (2020). https://doi.org/10.1016/j.jallcom.2020.154388
32. Mallesh, S., Srinivas, V., Vasundhara, M., Kim, K.H.: Low-temperature magnetization behaviors of superparamagnetic MnZn ferrites nanoparticles. Phys. B Condens. Matter. **582**, 411963 (2019). https://doi.org/10.1016/j.physb.2019.411963